

# Stoichiometry and Bravais lattice diversity: An *ab initio* study of the GaSb(001) surface

O. Romanyuk\*

*Paul-Drude-Institut für Festkörperelektronik, Hausvogteiplatz 5-7, D-10117 Berlin, Germany  
and Institute of Physics, Academy of Sciences of the Czech Republic, Cukrovarnická 10, 162 00 Prague, Czech Republic*

F. Grosse and W. Braun

*Paul-Drude-Institut für Festkörperelektronik, Hausvogteiplatz 5-7, D-10117 Berlin, Germany  
(Received 25 September 2008; revised manuscript received 30 April 2009; published 25 June 2009)*

We study the family of GaSb(001)-(4×3) reconstructions by *ab initio* density-functional theory. For each possible surface stoichiometry between the well-known Sb-poor  $\alpha(4\times 3)$  and Sb-rich  $\beta(4\times 3)$  phases, we find thermodynamically stable reconstructions. Surface energies of (4×3) unit cells shifted relative to each other are computed for the thermodynamically stable phases. Especially, the energetic costs for unit-cell shifts along the  $[\bar{1}10]$  direction with the length of one in-plane surface lattice constant are very low. In a comparative study, we show that this is similar to the  $\beta 2(2\times 4)$  reconstructed GaAs(001) surface with a one-dimensional disorder along  $[\bar{1}10]$ , but different from the  $c(4\times 4)$  reconstruction. The diversity in surface stoichiometry and unit-cell shape allows us to explain the contradicting experimental results obtained by scanning tunneling microscopy and surface-diffraction techniques at finite substrate temperatures.

DOI: 10.1103/PhysRevB.79.235330

PACS number(s): 68.35.B-, 68.35.Md, 68.47.Fg, 71.15.Mb

## I. INTRODUCTION

The epitaxial growth mode of III-V semiconductors can be controlled by varying the fluxes and the substrate temperature. This allows us to directly influence the atomic surface configuration. The number of known stable surface reconstructions of III-V compounds has grown rapidly within the last two decades.<sup>1,2</sup> The combination of scanning tunneling microscopy (STM) and structure calculations based on density-functional theory (DFT) has played a very important role in the surface structure identification. However, despite significant progress in the field, there are still a number of experimentally observed structures which are unresolved or in debate.

Particularly, one such puzzle is the appearance of certain unit-cell symmetries, which are spatially resolved by STM and found to be stable by DFT but are different from observed diffraction symmetries in reflection high-energy electron diffraction (RHEED) or x-ray diffraction. An important example is the GaAs(001)-(2×4) surface, which produces a (1×4) diffraction symmetry<sup>3,4</sup> with diffuse 2× intensity streaks. This can be explained by random unit-cell shifts of the (2×4) unit cells along the 2× direction. Another example are the GaSb(001)-(4×3) reconstructions, producing (1×3) or  $c(2\times 6)$  diffraction symmetry.<sup>5</sup> A possible explanation for this effect is the coexistence of several rectangular and oblique Bravais lattices or one-dimensional disorder on a surface within the coherence length of the diffraction beam. This may lead to the extinction of certain nonbulk reflections.<sup>6</sup> A theoretical model, in order to capture this effect, has to correctly describe statistical properties, mainly the correlation between shifted unit cells. Therefore, the interaction energy between cells with different unit-cell stoichiometries as well as different Bravais lattice types needs to be determined. A direct treatment of this problem within DFT is numerically difficult due to the large system size, especially if a larger number of different unit cells coexist on

the surface. Some progress has already been made in describing entropy effects in surface statistics on the basis of DFT calculations: diversity of heterodimer motifs within surface unit cell was considered.<sup>7</sup> For certain materials, however, one-dimensional disorder becomes an essential element of surface structure, and it should be included into the analysis. For instance, the GaAs(001)-(2×4) reconstruction with one-dimensional disorder<sup>2</sup> can be interpreted as a coexistence of “disorder free” (2×4) and  $c(2\times 8)$  reconstructions.

In the following, we use DFT to calculate changes in the total energy of a system due to distortion in the unit-cell translation periodicity to understand the underlying mechanisms of such distortions. The thermodynamics of GaSb(001) surface reconstructions is investigated. This includes changes in the unit-cell stoichiometry through the formation of heterodimers inside the cell as well as Bravais lattice diversity. A well suited system to study these effects is the family of (4×3) reconstructions: STM reveals characteristic surface defects on these surfaces including the coexistence of rectangular and oblique translation symmetries and various heterodimer configurations within one unit cell.<sup>8</sup> On the other hand, GaSb(001) is an important substrate surface for device growth in the 6.1 Å lattice-constant family of compounds (InAs, GaSb, AlSb, and ZnTe) and its surface reconstruction is important to understand disorder at the non-common anion interfaces.<sup>9</sup>

Different symmetry families can be observed by RHEED on GaSb(001) irradiated by a stationary  $Sb_4$  flux. The (1×3) diffraction pattern<sup>10,11</sup> can be explained using (4×3) unit cells in a model with preferential unit-cell shifts along the  $[\bar{1}10]$  azimuth.<sup>5</sup> The (4×3) unit cell is also confirmed to be thermodynamically stable by DFT.<sup>12,13</sup> The observed  $c(2\times 6)$  symmetry at lower substrate temperatures<sup>14</sup> belongs to the same symmetry family. The origin of the observed (1×5) pattern is still in debate<sup>15,16</sup> also with respect to thermodynamic stability.<sup>13,17</sup> Additionally, a  $c(2\times 10)$  periodicity is reported.<sup>11,15</sup>

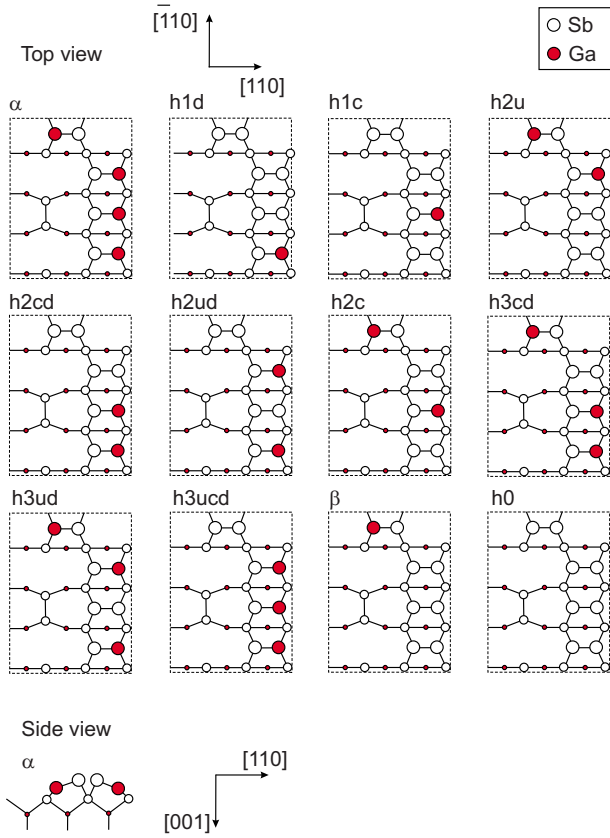


FIG. 1. (Color online) Structure models of different GaSb(001)- $(4 \times 3)$  reconstructions. Models with different stoichiometry are formed by substituting four Ga atoms in the top dimers of the  $\alpha$  model by Sb atoms. Equivalent structures obtained by mirror symmetry along  $[110]$  are not shown. Open (filled) spheres correspond to Sb (Ga) atoms. Model notation includes number of heterodimers  $h$  and heterodimer position within a dimer row: up ( $u$ ), center ( $c$ ), and down ( $d$ ) site.

The paper is organized as follows. In Sec. II we introduce the list of investigated structures including possible Bravais lattice types. The computational details are given in Sec. III, followed by the Results section in which we present GaSb(001)- $(4 \times 3)$  stable reconstructions, calculate the surface energies, and discuss possible effects caused by a one-dimensional disorder on a surface.

## II. $(4 \times 3)$ SURFACE RECONSTRUCTIONS

The  $(4 \times 3)$  structures observed by STM agree with DFT simulations for the  $\alpha$ ,  $\beta$ , and  $\gamma$  phases.<sup>8</sup> The  $\alpha$  phase involves four Ga-Sb dimers on top of an Sb layer (Fig. 1,  $\alpha$ ). The  $\beta$  phase is more Sb rich and it has three top Sb-Sb dimers and one Sb-Ga dimer (Fig. 1,  $\beta$ ). The  $\gamma$  ( $4 \times 3$ ) phase is the most Sb rich. It has four Sb-Sb dimers in the top layer of the surface within an oblique unit cell.

The extinction or the weakening of reflections which would be expected from a periodic arrangement of the same surface unit cell is caused by the loss of correlation, i.e., the violation of the perfect translational periodicity. This may be due to differences between the unit cells, such as the replace-

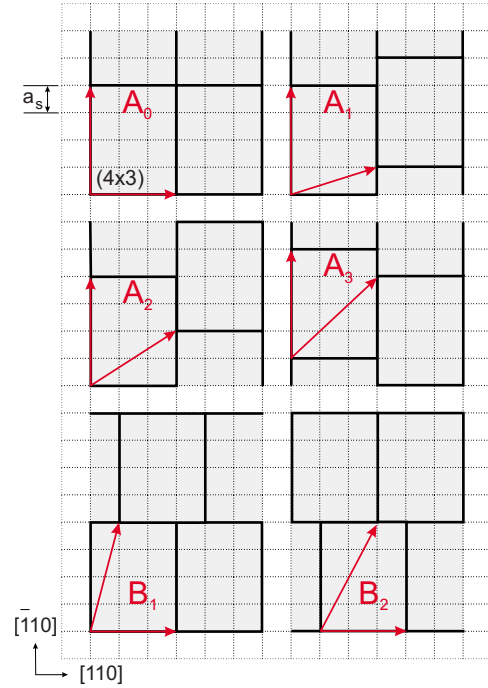


FIG. 2. (Color online) Schematic view of different unit-cell translation vectors to combine  $(4 \times 3)$  unit cells. The  $A_0$  case corresponds to orthogonal translation vectors. The  $A_1$ ,  $A_2$ ,  $A_3$ ,  $B_1$ , and  $B_2$  cases are oblique lattices. The surface lattice constant is  $a_s = a_{bulk}/\sqrt{2}$ , where  $a_{bulk}$  is the bulk lattice constant of GaSb.

ment of a Sb-Sb homodimer by a Ga-Sb heterodimer, or due to different Bravais lattice types, or both. As mentioned already in the Introduction, although the  $(4 \times 3)$  phases are the most energetically favorable for the GaSb(001) surface, the  $(4 \times 3)$  diffraction patterns are not observed in a diffraction experiment. The structure models that had been suggested earlier for the observed  $(1 \times 3)$  (Ref. 10) and  $c(2 \times 6)$  (Ref. 18) symmetries were not confirmed to be stable<sup>12,19</sup> by DFT calculations: the suggested structures have a higher surface energy than the different stable  $(4 \times 3)$  reconstructions.

To study possible distortions of the long-range periodicity, we analyze differences between the type and the arrangement of the top dimers within the  $(4 \times 3)$  unit cell. A diversity in arrangement of homodimer and heterodimer motifs within one unit cell was also observed for the GaAs(001)- $c(4 \times 4)$  reconstruction.<sup>20</sup> In the case of GaSb(001)- $(4 \times 3)$ , we consider the different arrangements as sketched in Fig. 1. Sixteen structure models can be composed by substituting the four heterodimers of the Sb-poor  $\alpha$  model by Sb homodimers up to the Sb-rich  $h0$  model.<sup>12</sup> The number is reduced to 12 inequivalent models because of a mirror plane along the  $[110]$  axis. Since phases with center positions of the top heterodimers occupied by Ga have never been observed by STM, these configurations are excluded from the analysis.

In addition, we consider a unit-cell translation diversity. For the  $(4 \times 3)$  unit-cell basis, we use the following translation symmetries (see Fig. 2): the rectangular lattice is marked by  $A_0$ . Oblique lattices are denoted by  $A_1$ ,  $A_2$ , and  $A_3$  with unit-cell shifts along  $[\bar{1}10]$  by 1, 2, or  $3a_s$ , respectively. The  $B_1$  and  $B_2$  lattices correspond to unit-cell shifts along  $[110]$

by 1 or  $2a_s$ , respectively. For instance, the stable  $\gamma(4 \times 3)$  reconstruction is obtained by starting from configuration  $h0$  of Fig. 1 and applying the translation vectors  $B_1$  in Fig. 2. Such unit-cell variations have been shown before to explain disorder effects in diffraction intensities,<sup>21,22</sup> as well as changes in the symmetry of diffraction patterns.<sup>3,4,23</sup>

### III. COMPUTATIONAL DETAILS

The unit cells discussed in the previous section are used as input for total-energy calculations within DFT. The ABINIT computer code is used to carry out the calculations.<sup>24,25</sup> We use the local-density approximation for the exchange-correlation energy functional. Norm-conserving pseudopotentials<sup>26</sup> of the Troullier-Martins type<sup>27</sup> are used to describe the atomic species. The electronic wave functions are expanded in a plane-wave basis with a converged kinetic-energy cutoff of 12 Ha and a  $\mathbf{k}$ -point set corresponding to  $3 \times 4$  points per  $(4 \times 3)$  surface Brillouin zone.<sup>28</sup> By applying the different translation vectors of Fig. 2, it is not possible to define an equivalent  $\mathbf{k}$ -point mesh. Nevertheless, we estimate the relative numerical error to be less than 1 meV per  $(1 \times 1)$  surface unit cell based on tests with an increased cutoff energy as well as higher-density  $\mathbf{k}$ -point meshes. The surface structures are constructed using the repeated supercell approach with a GaSb (GaAs) slab thickness of nine atomic layers, using equilibrium lattice parameters computed from the bulk GaSb,  $a_{\text{bulk}} = 5.96 \text{ \AA}$ , and the bulk GaAs,  $a_{\text{bulk}} = 5.33 \text{ \AA}$ . A vacuum gap thickness of 15  $\text{\AA}$  is used. The bottom surface of the slab is passivated by pseudo-hydrogens.<sup>29</sup> Atomic coordinates are adjusted until the interatomic forces become smaller than  $0.008 \text{ eV/\AA}$ , whereby only the three bottom layers (Sb-Ga-pseudo H) are kept fixed.

The total energies produced by the DFT calculations can be analyzed in two different ways. First, as is standard for the determination of stable surface reconstructions, the surface-energy density  $\gamma$  is computed by<sup>30</sup>

$$\gamma S = E_{\text{tot}} - (n_{\text{Sb}} - n_{\text{Ga}})\mu_{\text{Sb}} - n_{\text{Sb}}\mu_{\text{GaSb}}^{\text{bulk}}, \quad (1)$$

where  $E_{\text{tot}}$  is the total energy of system,  $\mu_i$  is the chemical potential of species  $i$ ,  $n_i$  is the number of the atoms in the cell, and  $S$  is the surface area. The experimental conditions are simulated by varying the chemical potential  $\mu_{\text{Sb}}$  in the thermodynamically allowed range  $-H_f < \mu_{\text{Sb}} - \mu_{\text{Sb}}^{\text{bulk}} < 0$ , where  $H_f$  is the heat of formation,  $H_f = \mu_{\text{Ga}}^{\text{bulk}} + \mu_{\text{Sb}}^{\text{bulk}} - \mu_{\text{GaSb}}^{\text{bulk}}$ . The  $\mu_{\text{Ga}}^{\text{bulk}}(\mu_{\text{Sb}}^{\text{bulk}})$  chemical potentials are computed for the orthorhombic  $\alpha$ -Ga (Ref. 31) and rhombohedral Sb phases, respectively. The Sb-rich and Ga-rich conditions correspond to  $(\mu_{\text{Sb}} - \mu_{\text{Sb}}^{\text{bulk}})/H_f = 0$  and  $(\mu_{\text{Sb}} - \mu_{\text{Sb}}^{\text{bulk}})/H_f = 1$ , respectively.

Second, assuming that there is only a nearest-neighbor interaction between adjacent unit cells, the line energy  $E_l$  per unit length of the unit-cell boundary can be extracted from the DFT calculations by the expression

$$E_l = \frac{E_{\text{tot}}(i) - E_{\text{tot}}(A_0)}{2a_{sp}}, \quad (2)$$

where  $E_{\text{tot}}(i)$  is the computed total energy of a slab with  $i$  running over the oblique translational symmetries (Fig. 2).  $p$

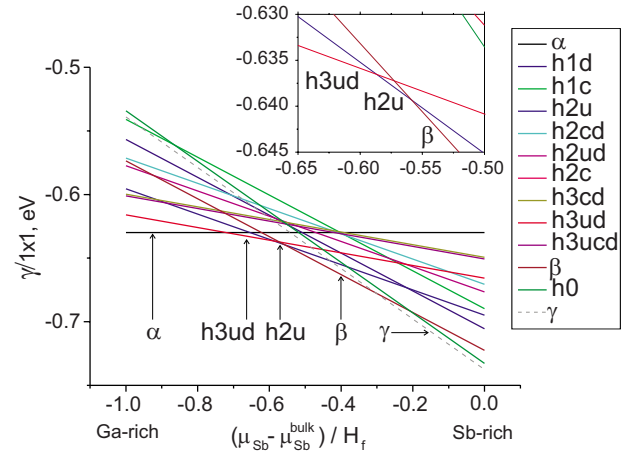


FIG. 3. (Color online) Surface-energy diagram of the GaSb(001)  $(4 \times 3)$  phases shown in Fig. 1. In the direction of increasing Sb flux, the following phases have the lowest energy:  $\alpha$  with four heterodimers,  $h3ud$  with three heterodimers,  $h2u$  with two heterodimers,  $\beta$  with one heterodimer, and finally  $\gamma$  with homodimers only and oblique surface lattice (Fig. 2,  $B_1$ ).

is 4 (3) for  $4 \times (3 \times)$  directions, respectively. The surface lattice constant is  $a_s = a_{\text{bulk}}/\sqrt{2}$ . Thus, a negative value of  $E_l$  corresponds to a reduction in the surface energy due to the oblique translation symmetry.

### IV. RESULTS AND DISCUSSION

The stability diagram presented in Fig. 3 for the different  $(4 \times 3)$  unit cells of Fig. 1 demonstrates that for every possible stoichiometry between the  $\alpha$  (four top heterodimers) and the  $\gamma$  reconstruction (zero heterodimers) a stable configuration is found. With decreasing number of top heterodimers,  $\alpha \rightarrow h3ud \rightarrow h2u \rightarrow \beta \rightarrow \gamma$  are found to be stable. The total energy of the  $h2u$  phase was found to be close to the total energy of the  $\beta$  phase.<sup>12</sup> Our calculation confirms that this phase is thermodynamically stable only in a very narrow chemical-potential range. The  $h3ud$  reconstruction extends previous results.<sup>12,13</sup> Therefore a smooth transition within the  $(4 \times 3)$  symmetry is possible which gradually increases the Sb content of the surface with increasing Sb chemical potential  $\mu_{\text{Sb}}$ . This is similar to reducing the temperature in the experiment. An analogous behavior is observed experimentally<sup>20</sup> and confirmed by DFT (Ref. 7) on the GaAs(001) surface for the  $c(4 \times 4)$  reconstructions. Phases with different numbers of heterodimer and homodimer within the unit cell with  $c(4 \times 4)$  symmetry were found to have a significant concentration at finite temperature in thermodynamic equilibrium. Thus, the behavior observed for the GaAs(001)  $c(4 \times 4)$  surface may be a rather common feature of III-V semiconductor surfaces. One reason is that the switching from homodimer to heterodimer does not change the electron number entering the electron counting rule.<sup>32</sup>

Furthermore, interactions between adjacent unit cells have to be included in a complete analysis. The interaction energy between adjacent  $c(4 \times 4)$  unit cells with different stoichiom-

TABLE I. Differences in energy  $E_i$  between unshifted and shifted unit-cell arrangements of the GaSb(001)-(4×3) and of the GaAs(001)- $\beta$ 2(2×4) and - $c$ (4×4) reconstructions.  $A_i$  and  $B_i$  represent unit-cell shifts by  $i$  surface lattice constants  $a_s$  along  $[\bar{1}10]$  and  $[110]$  directions, respectively (Fig. 2). The values are derived using Eq. (2) and are given in meV/Å. The differences in energy for GaSb(001)  $\alpha$  and  $\beta$ (4×3) with  $A_1$  lattice are smaller than the GaAs(001)- $\beta$ 2(2×4)- $A_1$  case.

	$A_1$	$A_2$	$A_3$	$B_1$	$B_2$	$B_3$
GaSb(001)-(4×3)						
$\alpha$	0.5	2	0.5	11	32	
$h3ud$	1	2	1	12	32	
$h2u$	0.9	2	0.5	13	27	
$\beta$	0.2	2	0.2	69	84	
$h0$	0.3	3	0.3	-2	12	
GaAs(001)						
$\beta$ 2(2×4)	0.7			24	33	24
$c$ (4×4)	20	30	20	85	72	85

eries was found to be small [ $<16$  meV/(1×1)] for GaAs(001).<sup>7</sup> For the GaSb(001)-(4×3) surface, Bravais lattice diversity is very common unlike for the GaAs(001)- $c$ (4×4) reconstruction. This leads to the conclusion that for the GaSb(001)-(4×3) surfaces, the interaction energies between shifted adjacent unit cells are smaller than for the unshifted GaAs(001)- $c$ (4×4) unit cells with different stoichiometries. To confirm this, we consider homogenous phases, i.e., the same stoichiometry within each GaSb(001)-(4×3) unit cell, but with different unit-cell translation vectors (see Fig. 2). In addition, we carry out calculations for the GaAs(001)- $\beta$ 2(2×4) and - $c$ (4×4) reconstructions to quantify the differences.

Within the supercell approach used here, changes in total energy due to a unit-cell translation distortion are interpreted as the change in interaction energy of two neighboring unit cells. The  $A_0$  type of translation corresponds to a rectangular Bravais lattice. Cases  $A_1$  and  $A_3$  correspond to  $1a_s$  and  $3a_s$  unit-cell shifts, along the  $[\bar{1}10]$  direction, respectively. Both structures can be symmetrically equivalent: the translational symmetry  $A_1$  is equivalent to  $A_3$  for  $\alpha$  but is not for  $h2u$ . In the same way,  $B_1$  and  $B_2$  denote  $1a_s$  and  $2a_s$  translations along the  $[110]$  azimuth. Thus, former unit cells are oblique with a cell area equal to the area of the rectangular (4×3) unit cell. Depending on the unit-cell translation periodicity, the local environment of the top as well as the trench dimers is changed. This results in changes in the total energy of the system.

In the case of the  $c$ (4×4) phase, a double rectangular unit cell with (4×4) size is used to accommodate all possible unit-cell shifts. Thus,  $A_{1,2,3}$  and  $B_{1,2,3}$  translations correspond to 1, 2,  $3a_s$  shifts of three top dimers relative to the neighboring top dimers along the  $[\bar{1}10]$  and the  $[110]$  directions, respectively.

In Table I, the energy differences between rectangular and oblique configurations,  $E_i$ , are listed in meV/Å units [Eq.

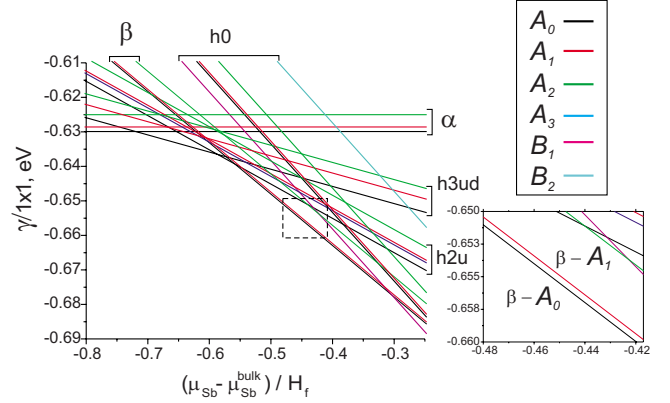


FIG. 4. (Color online) Surface-energy diagram of the most favorable GaSb(001)-(4×3) phases with rectangular ( $A_0$ ) and oblique ( $A_1$ ,  $A_2$ ,  $A_3$ ,  $B_1$ , and  $B_2$ ) surface translation vectors (Fig. 2). The structures  $\alpha$ ,  $h3ud$ ,  $h2u$ ,  $\beta$ , and  $h0$  are defined in Fig. 1. In order to emphasize the small energy differences, only a selected region of chemical potential,  $(\mu_{\text{Sb}} - \mu_{\text{Sb}}^{\text{bulk}})/H_f$ , is shown. The combinations of two  $\beta$ (4×3) cells with rectangular ( $A_0$ ) and oblique ( $A_1$ ) translation vectors have the smallest surface-energy difference equal to 0.6meV per (1×1) cell. The area within the dashed rectangle is magnified on the right-hand insert.

(2)]. All oblique configurations are energetically less favorable than the rectangular configuration, except for the  $\gamma$  phase ( $h0-B_1$ ). The energy differences, however, are small for the  $A_1$  and the  $A_3$  cases for the stable phases ( $\alpha$ ,  $h2u$ ,  $h3ud$ , and  $\beta$ ). Doubling the unit-cell shift, such as in configuration  $A_2$ , increases the energy by an order of magnitude. Even larger energies are found for the  $B_1$  and the  $B_2$  configurations, except for the  $\gamma$  phases as mentioned already.

Interaction energies for the GaSb(001)-(4×3) reconstruction can be directly compared with GaAs(001) reconstruction energies. For the  $\beta$ 2(2×4)- $A_1$  reconstruction with a shift in the  $2\times$  direction [ $c$ (2×8) unit cell], we find a somewhat higher interaction energy ( $E_i=0.7$  meV/Å) as for the GaSb(001)- $\beta$ (4×3)- $A_1$  ( $E_i=0.2$  meV/Å) and - $\alpha$ (4×3)- $A_1$  ( $E_i=0.5$  meV/Å) surfaces. All other values are significantly larger for shifts along the  $[110]$  direction. We therefore conclude that one-dimensional disorder is unlikely in this direction.

In Fig. 4, the surface-energy differences of five stable GaSb(001)-(4×3) phases (Fig. 3) with different translation symmetries (Fig. 2) are shown. Only a limited region of chemical potential and surface energy is plotted in order to resolve the small changes in surface energy. In case of the  $\alpha$  phase stoichiometry, the energy difference between the rectangular  $A_0$  and the oblique  $A_1$  lattices is about 1 meV per (1×1) cell. For the  $\beta$  phase, the difference is even smaller and equal to 0.6 meV per (1×1). The phases  $h3ud$  and  $h2u$  show a similar behavior [3 and 2 meV per (1×1), respectively]. Due to these small energy differences, unit-cell shifts are likely to occur at finite temperatures. The difference in surface energy is then correlated with the probability of a certain Bravais lattice. Therefore, it is expected that rectangular unit cells,  $A_0$ , are simultaneously present with oblique lattices of  $A_1$  and  $A_3$  types in thermodynamical equilibrium.

One possible reason for such a Bravais lattice diversity may be the structure of the surface unit cell itself. A unit-cell

shift increases the total energy of the system but this energy increase can be minimized by atomic relaxation. In particular, the GaAs- $\beta 2(4 \times 3)$  as well as the GaSb- $(4 \times 3)$  unit cells consist of a few reconstructed atomic layers with trench dimers in the third and in the second atomic layers, respectively. In both cases these trench dimers are oriented along  $[\bar{1}10]$ . This may compensate the stress caused by the unit-cell shifts: the lattices have more degrees of freedom to relax. A similar possibility to compensate stress may also exist on Sb terminated InAs(001),<sup>33</sup> where an apparent  $(2 \times 8)$  unit cell is confirmed by STM and DFT calculations but appears only as a  $\times 8$  diffraction pattern. In this case even four atomic layers including a trench contribute to the surface reconstruction. The GaAs(001)- $c(4 \times 4)$  reconstruction, however, has only one missing atomic row in the second layer without dimers. Thus, the latter structure is more rigid and the total energy increases significantly with unit-cell shifts.

Unit-cell shifts are observed by STM for GaSb- and AlSb- $\alpha$  and  $-\beta(4 \times 3)$  reconstructions,<sup>8</sup> and for the GaAs(001)- $\beta 2(4 \times 3)$  phase.<sup>2</sup> Single step unit-cell shifts along  $[\bar{1}10]$  can be recognized. Such shifts are not observed for  $c(4 \times 4)$  reconstructions. This agrees with the interaction energies presented in Table I. It also explains the symmetry of the diffraction pattern: the  $4 \times$  reflections vanish due to the broken periodicity along the  $4 \times$  direction for the  $(4 \times 3)$  unit cell. The results support our previous treatment, where interaction energies between shifted unit cells were assumed negligibly small.<sup>5</sup> Finally, small energy differences may lead to an oblique Bravais lattice at elevated temperature, whereas the analysis at zero temperature (Fig. 4) suggests that the stable reconstructions have rectangular symmetry.

A nonzero value of the line energy  $E_l$ , however, will impose an upper bound on the length of the shifted unit-cell rows. The gain in energy due to the interaction of two shifted unit cells can be compensated by step edges or defects. The  $\gamma$  phase is unique among the  $(4 \times 3)$  reconstructions. It has an oblique unit cell, and several coexisting phases (i.e., a mixture of  $h0$ ,  $h0-A_1$ , and  $\gamma$ ) are likely at higher temperature with fixed chemical potential. In this case, additional defects such as antiphase boundaries are necessary to accom-

modate the rectangular and the oblique lattices. This includes, e.g., possible changes in the number of top dimers within a cell. Qualitatively, if such defects are energetically unfavorable, they may exist in non-negligible quantities only in a nonequilibrium situation like growth. An analysis including these defects is obviously necessary but beyond the scope of the paper. It should be emphasized that such surface defects will change the surface unit-cell area, a case we did not treat here. Nevertheless, the current results demonstrate that the surface can easily accommodate such a defect-induced symmetry change by introducing low-energy shifts within an arrangement of  $(4 \times 3)$  unit cells. If the defect had a low energy it would not alter the findings significantly. Only where defects are necessary, such as in the  $\gamma$  phase, they may play a more important role.

## V. CONCLUSIONS

We have studied various GaSb(001)- $(4 \times 3)$  reconstructions with different unit-cell stoichiometries as well as various Bravais lattices by DFT. Thermodynamically stable reconstructions are found for all possible stoichiometries by exchanging the Ga and the Sb atoms in the top heterodimers of the  $\alpha(4 \times 3)$  structure as shown in Fig. 1. We have found two intermediate thermodynamically stable phases between the  $\alpha$  and the  $\beta(4 \times 3)$  phases: the  $h2u$  and the  $h3ud$  structures with two and three Sb-Ga dimers on the surface, respectively. The  $h2u$  structure exists only in a very narrow chemical-potential range. Deviations from a rectangular cell lead to only slightly higher energies for all stable reconstructions except for  $\gamma$ . Small energy differences between  $(4 \times 3)$  unit cells with rectangular and oblique translation symmetries should lead to one-dimensional disorder at nonzero temperature. This agrees with previous experimental results obtained by STM and explains the apparent contradiction in unit-cell symmetry observed by STM and by diffraction techniques.

## ACKNOWLEDGMENTS

Special thanks go to V. M. Kaganer for useful discussions and Petr Ryšavý for technical assistance. Support by German Research Foundation (Grant No. GZ: 436 TSE 113/62/0-1) and Institute of Physics, the Academy of Sciences of the Czech Republic (the Institutional Research Plan No. AVOZ 10100521 and LUNA project) is gratefully acknowledged.

\*romanyuk@fzu.cz

<sup>1</sup>W. G. Schmidt, Appl. Phys. A: Mater. Sci. Process. **75**, 89 (2002).

<sup>2</sup>A. Ohtake, Surf. Sci. Rep. **63**, 295 (2008).

<sup>3</sup>B. A. Joyce, J. H. Neave, P. J. Dobson, and P. K. Larsen, Phys. Rev. B **29**, 814 (1984).

<sup>4</sup>P. K. Larsen and D. J. Chadi, Phys. Rev. B **37**, 8282 (1988).

<sup>5</sup>O. Romanyuk, V. M. Kaganer, R. Shayduk, B. P. Tinkham, and W. Braun, Phys. Rev. B **77**, 235322 (2008).

<sup>6</sup>*Low-Energy Electron Diffraction: Experiment, Theory, and Structure Determination*, edited by M. A. V. Hove, W. H. Weinberg, and C. M. Chan (Springer-Verlag, Berlin, 1986), Vol. 6.

<sup>7</sup>E. Penev, P. Kratzer, and M. Scheffler, Phys. Rev. Lett. **93**, 146102 (2004).

<sup>8</sup>W. Barvosa-Carter, A. S. Bracker, J. C. Culbertson, B. Z. Noshov, B. V. Shanabrook, L. J. Whitman, H. Kim, N. A. Modine, and E. Kaxiras, Phys. Rev. Lett. **84**, 4649 (2000).

<sup>9</sup>B. Z. Noshov, W. H. Weinberg, W. Barvosa-Carter, B. R. Bennett, B. V. Shanabrook, and L. J. Whitman, Appl. Phys. Lett. **74**, 1704 (1999).

<sup>10</sup>A. S. Bracker, M. J. Yang, B. R. Bennett, J. C. Culbertson, and W. J. Moore, J. Cryst. Growth **220**, 384 (2000).

<sup>11</sup>M. T. Sieger, T. Miller, and T.-C. Chiang, Phys. Rev. B **52**, 8256 (1995).

- <sup>12</sup>M. C. Righi, R. Magri, and C. M. Bertoni, *Phys. Rev. B* **71**, 075323 (2005).
- <sup>13</sup>J. Houze, S. Kim, S.-G. Kim, S. C. Erwin, and L. J. Whitman, *Phys. Rev. B* **76**, 205303 (2007).
- <sup>14</sup>U. Resch-Esser, N. Esser, B. Brar, and H. Kroemer, *Phys. Rev. B* **55**, 15401 (1997).
- <sup>15</sup>L. J. Whitman, P. M. Thibado, S. C. Erwin, B. R. Bennett, and B. V. Shanabrook, *Phys. Rev. Lett.* **79**, 693 (1997).
- <sup>16</sup>B. P. Tinkham, O. Romanyuk, W. Braun, K. H. Ploog, F. Grosse, T. Takahasi, T. Kaizu, and J. Mizuki, *J. Electron. Mater.* **37**, 1793 (2008).
- <sup>17</sup>O. Romanyuk, W. Braun, and F. Grosse, *e-J. Surf. Sci. Nanotechnol.* **7**, 429 (2009).
- <sup>18</sup>F. Maeda, Y. Watanabe, and M. Oshima, *J. Electron Spectrosc. Relat. Phenom.* **80**, 225 (1996).
- <sup>19</sup>K. Chuasiripattana and G. P. Srivastava, *Surf. Sci.* **600**, 3803 (2006).
- <sup>20</sup>A. Ohtake, P. Kocan, J. Nakamura, A. Natori, and N. Koguchi, *Phys. Rev. Lett.* **92**, 236105 (2004).
- <sup>21</sup>Y. Garreau, M. Sauvage-Simkin, N. Jedrecy, R. Pinchaux, and M. B. Veron, *Phys. Rev. B* **54**, 17638 (1996).
- <sup>22</sup>M. Takahasi, Y. Yoneda, N. Yamamoto, and J. Mizuki, *Phys. Rev. B* **68**, 085321 (2003).
- <sup>23</sup>T. Abukawa, T. Okane, and S. Kono, *Surf. Sci.* **256**, 370 (1991).
- <sup>24</sup>The ABINIT code is a common project of the Université Catholique de Louvain, Corning Incorporated, and other contributors, [www.abinit.org](http://www.abinit.org)
- <sup>25</sup>X. Gonze, J.-M. Beuken, R. Caracas, F. Detraux, M. Fuchs, G.-M. Rignanese, L. Sindic, M. Verstraete, G. Zerah, F. Jollet, M. Torrent, A. Roy, M. Mikami, Ph. Ghosez, J.-Y. Raty, and D. C. Allan, *Comput. Mater. Sci.* **25**, 478 (2002).
- <sup>26</sup>M. Fuchs and M. Scheffler, *Comput. Phys. Commun.* **119**, 67 (1999).
- <sup>27</sup>N. Troullier and J. L. Martins, *Phys. Rev. B* **43**, 1993 (1991).
- <sup>28</sup>H. J. Monkhorst and J. D. Pack, *Phys. Rev. B* **13**, 5188 (1976).
- <sup>29</sup>K. Shiraishi, *J. Phys. Soc. Jpn.* **59**, 3455 (1990).
- <sup>30</sup>C. Ratsch, W. Barvosa-Carter, F. Grosse, J. H. G. Owen, and J. J. Zinck, *Phys. Rev. B* **62**, R7719 (2000).
- <sup>31</sup>M. Bernasconi, G. L. Chiarotti, and E. Tosatti, *Phys. Rev. B* **52**, 9988 (1995).
- <sup>32</sup>M. D. Pashley, *Phys. Rev. B* **40**, 10481 (1989).
- <sup>33</sup>W. Barvosa-Carter, F. Grosse, J. H. G. Owen, and J. J. Zinck, *Progress in Semiconductor Materials for Optoelectronic Applications*, MRS Symposia Proceedings No. 692 (Materials Research Society, Pittsburgh, 2002), p. H8.4.1.